Focusing microwaves into subwavelength dimensions with a half-cylindrical hyperlens based on split ring resonators

Guoxing Zheng (郑国兴)[1*], Zile Li (李子乐)[1], Guishan Yuan (袁桂山)[2], Ruiying Zhang (张瑞瑛)[3], Ping'an He (何平安)[1], Xiaochun Dong (董小春)[2], Jun Cui (崔 钧)[1], Jiangnan Zhao (赵江南)[1], Jianping Yun (郧建平)[1], and Song Li (李 松)[1]

[1]*School of Electronic Information, Wuhan University, Wuhan 430072, China*

[2]*Institute of Optics and Electronics, Chinese Academy of Sciences, Chengdu 610209, China*

[3]*Department of Biomedical Engineering, Washington University in St. Louis, One Brookings Dr., St. Louis, Missouri, 63130, USA*

[*]*Corresponding author: gxzheng@whu.edu.cn*

Received March 28, 2014; accepted April 23, 2014; posted online July 18, 2014

Hyperlenses based on metamaterials can be applied to subwavelength imaging in the lightwave band. In this letter, we demonstrate both through simulations and experimentally verified results that our proposed half-cylindrical shaped hyperlens can be used for super-resolution microwave focusing in a TE mode. Based on split ring resonators, the hyperlens satisfies a hyperbolic dispersion relationship. Simulations demonstrate that the focused spot size and position are insensitive to the rotation angle of the hyperlens around its geometric center. Experimental results show that a focused spot size 1/3 of the vacuum wavelength is achieved in the microwave band.

OCIS codes: 160.3918, 350.4010, 350.5730.

doi: 10.3788/COL201412.081602.

In the lightwave band, a hyperlens made of alternating metallic and dielectric layers with a hyperbolic dispersion relationship has been analyzed theoretically[1] and verified by simulations and experiments[2−5]. Such a device has achieved both super-resolution imaging and magnification imaging. A typical optical hyperlens consists of tens or hundreds of curved metallic and dielectric layers only a few nanometers thick[2−6], whose radii are on the micrometer level. Fabricating such a device is difficult because of its ultra-small dimensions and multilayer structure. Furthermore, the inherent absorption loss of metals and unavoidable fabrication errors offset the device's extra high resolution because small perturbations are often strong enough to distort the delicate transformations of large wave vectors[6]. For the above reasons, it remains considerably challenging to manufacture hyperlenses for super-resolution imaging in the lightwave band.

Unlike the lightwave devices, microwave super-resolution imaging devices have dimensions on the millimeter or centimeter level, which can greatly reduce the fabrication and assembling requirements. In our former works, we have verified that an optical hyperlens can be employed for super-resolution beam focusing[7−9], just like many others metamaterials based devices[10,11]. In this letter, we propose a microwave beam-focusing hyperlens device based on split ring resonators (SRRs) and analyze its unique focusing-properties. This newly developed device may find applications in microwave catalysis[12], microwave synthesis[13], microwave medical devices[14,15], and other potential fields requiring microwave beam focusing.

Metamaterials can achieve the required equivalent dielectric constant ε and magnetic permeability μ through optimal design of the material structure[16,17]. A hyperlens made up of metamaterials with an optimized design can control the transmission properties of incident electromagnetic waves. In cylindrical coordinates, for the TE mode, the dispersion relationship of metamaterials satisfies

$$\frac{k_r^2}{\mu_\varphi} + \frac{k_\varphi^2}{\mu_r} = \omega^2 \varepsilon_z, \tag{1}$$

where k_r is the radial wavevector, k_φ is the angular wave vector, μ_φ and μ_r are the angular and radial magnetic permeabilities respectively, ω is the working wave frequency, and ε_z is the dielectric constant in the electric field direction. For harmonic magnetic resonance metamaterials (applicable in microwave bands), if $\mu_r < 0$, and $\mu_\varphi > 0$ (or both conversely), the dispersion equation denotes a hyperbolic curve. Under such circumstances, the modules of angular wave vectors which determine the resolution will not be restricted, unlike those of traditional materials with circular or elliptic dispersion equations. Object waves with angular wave vectors exceeding k_0, which represent the details of the object, can spread in the material in traveling wave modes instead of evanescent wave modes, allowing super resolution focusing and imaging in a far field. Furthermore, studies[18,19] have shown that, when $\mu_\varphi \to 0$ is satisfied, the dispersion curves of this material will degenerate into two lines parallel to the k_φ axis. Therefore, all rays will propagate in a direction parallel to k_r, so all waves incident on the material, regardless of the magnitude or the propagation direction of the wave vectors, will focus into the sphere center. As a result, a high energy density beam spot is produced beyond the diffraction. Relying on the above principles, we propose a microwave beam-focusing device based on metamaterials.

To verify super-resolution beam focusing in the microwave band, we have designed a microwave beam-focusing device with the basic structure shown in Fig.

1. This device is composed of an object stage, absorbing materials, a horn antenna, a dielectric lens, and a microwave hyperlens. A slab waveguide formed by two parallel metal plates receives the incident microwaves. The microwaves are expanded and collimated by the horn waveguide and then focused by a dielectric lens. Absorbing materials are evenly distributed around the measurement area. The phases and intensities of the focusing fields near the hyperlens' focal plane can also be measured by a microwave probe.

As shown in Fig. 1(a), we chose a horn antenna to expand the beam expansion of microwaves. In our design, a focusing dielectric lens transformed the collimated microwaves into convergent cylindrical waves that fit within the shape of the hyperlens. Without the dielectric lens, a large microwave hyperlens with more layers could be used, if it is large enough to include all the incident collimated microwaves. This design, however, would decrease the system's transmission efficiency and increase the fabrication difficulty. In addition, another benefit from the dielectric lens is that it can reduce the reflection loss at the boundary of the hyperlens. Without the dielectric lens, the marginal rays projected on the outmost layer of the hyperlens will encounter large incident angles at the medium boundary, which will cause a large Fresnel reflection loss. Fortunately, the dielectric lens ensures that each incident ray arrives on the hyperlens at normal incidence. Our former research[7] showed that with such a design, the transmission efficiency of an optical hyperlens beam focusing system can be improved from 0.1% to 5.3%.

The dielectric lens is made up of plano-convex lenses. The collimated microwave rays from the horn waveguide pass through the front surface of the dielectric lens perpendicularly and then are focused at the back surface. According to the aplanatic principle, an off-axis position (x, y) at the curve surface of the lens meets

$$f_1 + (n-1)\,d = \sqrt{(-x+f_1)^2 + y^2} + nx, \qquad (2)$$

and the on-axis point and edge point satisfy

$$f_1 + (n-1)d = \sqrt{f_1^2 + \left(\frac{D}{2}\right)^2}, \qquad (3)$$

where f_1 is the focal length, D is the aperture of the lens, d is the thickness of the lens, and n is the refractive index of the lens material. On the basis of Eqs. (2) and (3), we can get the required surface profile of the plano convex dielectric lens. In this design, the parameters of the lens are $D = 180$ mm, $f_1 = 180$ mm, $n = 1.5969$, and $d = 35.59$ mm.

As shown in Fig. 1(b), the microwave hyperlens is composed of periodic units of SRRs, and the parameters of the SRRs in Fig. 1(c) have been carefully designed to meet the hyperbolic dispersion equation requirement. The designed hyperlens is made up of 17 layers of periodic SRRs with layers separation of 2.7 mm, and the outer diameter is 100 mm. The substrate and metal material of the SRRs are FR-4 epoxy board and copper, respectively. Our SRRs have simple structure and magnetic resonance frequency that can be varied in a large range by changing the design parameter of SRRs; thus the μ_r and μ_ϕ which meet the needs can be obtained easily. That's the reason why we chose the TE wave instead of the TM wave.

Using HFSS software to make electromagnetic simulation on optimized SRRs, we can get its S-parameters to retrieve its effective permeability and effective permittivity, and then we can get its dispersion curve, as shown in Fig. 2. While the effective electromagnetic parameters of the hyperlens change smoothly when the microwave frequency f is at around 10 GHz, we take 10 GHz as a working frequency. The corresponding effective electromagnetic parameters are $\mu_r = -1.93$, and $\mu_\varphi = 0.86$. These parameters meet the requirement for a hyperbolic dispersion relationship, and thus the hyperlens can be used for super-resolution beam focusing.

In practice, the focal plane of the hyperlens is placed at the focal plane of the dielectric lens. In this way, the cylindrical shape of each layer of the hyperlens matches well with the wavefront of the convergent waves. Thus only the wavenumbers increase as the convergent waves propagate without perturbation of the wavefront.

Using the electromagnetic simulation software COMSOL^{TM} 4.2, the properties and super-resolution beam focusing ability of the proposed device were verified through simulations. Figure 3(a) shows the electric field distribution in the simulation domain. Though it shows high reflection in front of the hyperlens due to the impedance mismatch primarily, there is still an obvious focused spot in the focal plane. Figure 3(b) shows the intensity distributions of the focused microwave along the focal plane. As seen in Fig. 3(b), the full-width at half-maximum (FWHM) of the focused spot is about 8.6 mm (corresponding to $\lambda_0/3.5$, where λ_0 is the wavelength in vacuum). Without the hyperlens, the FWHM of the spot focused only by dielectric lens is no less than the diffractive limit $\lambda_0/2\text{NA}=1.1\lambda_0$. Here NA is defined as the numerical aperture of the dielectric lens and its value is approximately equal to $\sin[\tan^{-1}(D/2f_1)]$.

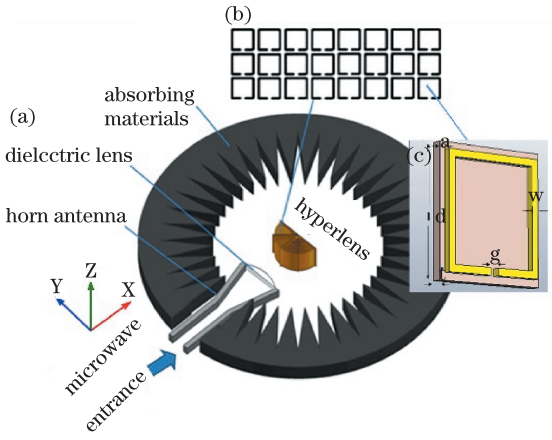

Fig. 1. (a) Schematic of the experimental device, (b) a sketch of the periodic arrangement of the split ring units in the layers (the pitch of each unit is 2.7 mm) and (c) a unit of the optimally designed SRR structure. The SRR is square with a substrate length $l = 2.7$ mm, substrate thickness $d = 0.25$ mm, metal thickness $t = 0.034$ mm, metal length $a = 2.4$ mm, metal width $w = 0.15$ mm, and gap width $g = 0.2$ mm.

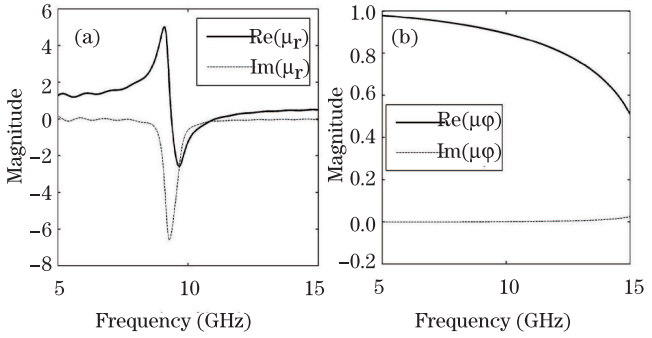

Fig. 2. (Dispersion curve of optimized SRRs with (a) retrieved effective permeability μ_r and (b) resumed effective permeability μ_ϕ.

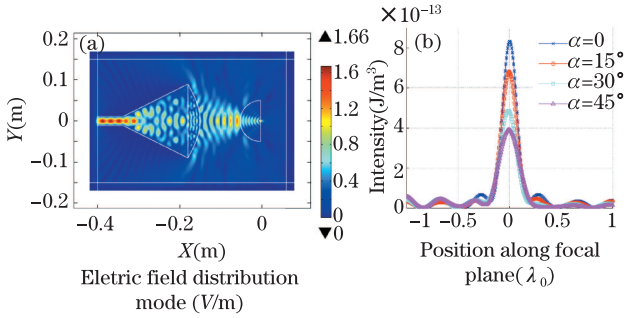

Fig. 3. (a) Electric field distribution mode in the simulation domain and (b) intensity distribution of the focused spots on the focal plane when the hyperlens rotates an angle α around its centre of sphere in the horizontal plane.

Therefore, the ability of the proposed device to focus its beam beyond the diffraction limit was confirmed by the simulation.

Simulation also showed that the hyperlens was not sensitive to incident angles. When the hyperlens rotates an angle α around the center of the sphere in the horizontal plane, the intensity distributions on the focal plane are shown in Fig. 3(b) with α equal to 0, 15°, 30°, and 45° degrees, respectively. According to Fig. 3(b), there are no significant fluctuations in the size of the focused spots or their positions, except for some energy loss at large incident angles. These findings are consistent with semi-classical theory[18], which states that all of the lights incident to the hyperlens will converge to the core of the sphere in spiral lines. Such a distinguishing feature can greatly reduce the assembly requirements of the hyperlens in practice. Additionally, problems in traditional microwave devices, such as degradation of the focusing quality caused by the deformation of the focusing wave, can be easily avoided in such a device.

The proposed beam-focusing system is shown in Fig. 4. Figure 4(a) is a schematic of the automatic 2D measuring system, which measures the field distribution of microwaves on the $x-y$ plane, controlled by a microcomputer. Figure 4(b) is our experimental system, and Fig. 4(c) is the hyperlens fabricated by circuit-board printing technology operating in the microwave band.

In the experiments, microwave signals were generated by a vector network analyzer, and frequencies were scanned between 8 to 12 GHz. These microwave signals were transmitted into the designed device and focused near the focal plane of the hyperlens. To discover the best operating wavelength, we scanned and recorded the microwave power flow distribution near the hyperlens' focal plane by using a microwave probe with a sampling interval of 0.1 mm. Data analysis verified that the best focusing effect appeared at the designed frequency of 10 GHz, which produced the smallest focused spots and least noise. The power flow distribution is shown in Fig. 5(a), where the focal plane of the hyperlens is marked by a red dashed line. The power flow distribution at the focal plane is shown in Fig. 5(b). According to Fig. 5(b), the measured FWHM of the focused spot is about 10 mm (corresponding to $\lambda_0/3$), which is close to the theoretical value of $\lambda_0/3.5$ and less than the diffraction limited spot size $1.1\lambda_0$. Besides the intrinsic loss of materials, manufacturing error of SRRs, distortions of layer curve, and probe detection error may also contribute to the small difference between the simulated and experimental spots dimension. By decreasing the separation between multi-layers of the hyperlens, optimizing the metamaterial unit structure, and improving the microwave collimating and focusing efficiency, the resolution of the beam-focusing

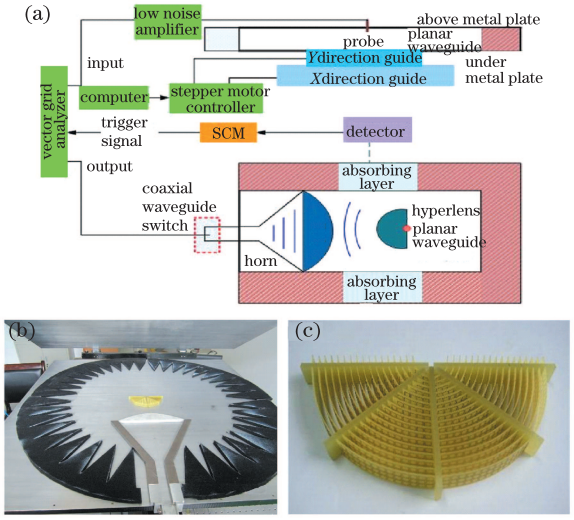

Fig. 4. (a) Schematic diagram of automatic 2D measuring system, photos of (b) the microwave focusing experiment setup and (c) the microwave hyperlens used in our experiment.

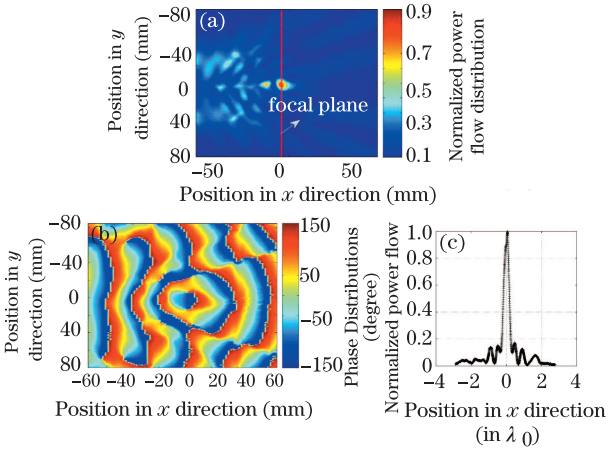

Fig. 5. (a) Experimental two-dimension microwave power flow distribution and phase, (b) distribution near the focal plane and (c) normalized power flow distribution at the focal plane.

device can be further improved experimentally.

It can also be seen from Fig. 5(a) that the microwaves diverge quickly after leaving the focal plane. The reason is that microwave components with transverse wave vectors larger than k_0 have been turned into evanescent waves after leaving the hyperlens. The evanescent waves experience an exponential attenuation of amplitudes, and the bigger the wave vectors, the faster the attenuation[8]. Therefore the working plane should be as close to the focusing device as possible in applications.

In summary, we present a microwave device combining a horn antenna, dielectric lenses, and a hyperlens to realize super-resolution focusing in the microwave band. A device layout is suggested and the device's characteristics are analyzed theoretically. Numerical simulations and experiments further verify our design and demonstrate that the minimum focusing spot size can be reduced to $\lambda_0/3$. To improve the performance of the system, we use a dielectric lens to transform the collimated microwaves into convergent cylindrical waves that fit within the shape of the hyperlens, which is different from other promising subwavelength imaging devices[19,20]. With a simple structure, a robustness to assembly variations, this newly proposed microwave device, when further optimized, is expected to find numerous applications in such fields as microwave catalysis, microwave synthesis, and medical treatment.

This work was supported by the National Natural Science Foundation of China under Grants Nos. 11374235, 61271150, 61007024, and 10904118. We appreciate Prof. James Ballard's close reading of the manuscript.

References

1. Z. Jacob, L. V. Alekseyev, and E. Narimanov, Opt. Express **14,** 8247 (2006).
2. Z. Liu, H. Lee, Y. Xiong, C. Sun, and X. Zhang, Science **315,** 1686 (2007).
3. I. I. Smolyaninov, Y. J. Hung, and C. C. Davis, Science **315,** 1699 (2007).
4. H. Lee, Z. Liu, Y. Xiong, C. Sun, and X. Zhang, Opt. Express **15,** 15886 (2007).
5. J. Rho, Z. L. Ye, Y. Xiong, X. B. Yin, Z. Liu, H. Choi,G. Bartal, and X. Zhang, Nat. Commun. **1,** 143 (2010).
6. X. Zhang and Z. Liu, Nat. Mater. **7,** 435 (2008).
7. G. Zheng, R. Zhang, S. Li, P. He, and H. Zhou, Chin. Phys. B **20,** 117802 (2011).
8. G. Zheng, R. Zhang, S. Li, P. He, H, Zhou, and Y. Shi, IEEE Photon. Techol. Lett. **23,** 1234 (2011).
9. J. Zhao, G. Zheng, S. Li, H. Zhou, Y. Ma, R. Zhang, Y. Shi, and P. He, Chin. Opt. Lett. **10,** 042302 (2012).
10. A. Ourir, G. Lerosey, F. Lemoult, M. Fink, and J. de Rosny, Appl. Phys. Lett. **101,** 111102 (2012).
11. A. Sentenac, P. C. Chaumet, and K. Belkebir, Phys. Rev. Lett. **97,** 243901 (2006).
12. S. G. Aitken and A. D. Abell, Aust. J. Chem. **58,** 3 (2005).
13. C. O. Kappe and D. Dallinger, Nat. Rev. Drug Discov. **5,** 51 (2006).
14. F. Sterzer, IEEE Microw. Mag. **3,** 65 (2002).
15. S. C. Hagness, E. C. Fear, and A. Massa, IEEE Antenn. Wireless Propag. Lett. **11,** 1592 (2012).
16. M. Zhong, Chin. Opt. Lett. **11,** 101601 (2013).
17. B. Na, J. Shi, C. Guan, and Z. Wang, Chin. Opt. Lett. **11,** 111602 (2013).
18. Z. Jacob, L. V. Alekseyev, and E. Narimanov, J. Opt. Soc. Am. A. **24,** 52 (2007).
19. W. Zhang, H. Chen, and H. O. Moser, Appl. Phys. Lett. **98,** 073501 (2011).
20. B. Zheng, R. Zhang, M. Zhou, W. Zhang, S. Lin, Z. Ni, H. Wang, F. Yu, and H. Chen, Appl. Phys. Lett. **104,** 073502 (2014).